International Journal of Mechanical, Industrial and Aerospace Sciences
ISSN: 2517-9950
Vol:3, No:1, 2009

Construction and Performance Characterization of the Looped-Tube Travelling-Wave Thermoacoustic Engine with Ceramic Regenerator

Abdulrahman S. Abduljalil, Zhibin Yu, Artur J. Jaworski, and Lei Shi

***Abstract*—**In a travelling wave thermoacoustic device, the regenerator sandwiched between a pair of (hot and cold) heat exchangers constitutes the so-called thermoacoustic core, where the thermoacoustic energy conversion from heat to acoustic power takes place. The temperature gradient along the regenerator caused by the two heat exchangers excites and maintains the acoustic wave in the resonator. The devices are called travelling wave thermoacoustic systems because the phase angle difference between the pressure and velocity oscillation is close to zero in the regenerator. This paper presents the construction and testing of a thermoacoustic engine equipped with a ceramic regenerator, made from a ceramic material that is usually used as catalyst substrate in vehicles' exhaust systems, with fine square channels (900 cells per square inch). The testing includes the onset temperature difference (minimum temperature difference required to start the acoustic oscillation in an engine), the acoustic power output, thermal efficiency and the temperature profile along the regenerator.

***Keywords*—**Regenerator, Temperature gradient, Thermoacoustic, Travelling-wave.

I. Introduction

IN the last few decades, the production of fossil fuels has increased dramatically to meet the ever increasing demand for energy that becomes the main indicator of the modern development of all countries. Although, the improvement of system efficiencies and energy saving processes are so effective for reducing the energy consumption, the growth of the world population tends to increase the demand for energy. With this dramatic increase in consumption, the prices of these non-renewable fuels continue to rise. Moreover, the pollution concern has become a worrying factor for the engineers to work on protecting the environment for future generations. This situation leads to the necessity of developing new technologies that are based on the utilization of renewable sources of energy and/or low temperature energy sources (waste heat). One of the promising technologies is thermoacoustic technology, which can work using relatively low temperature difference. In thermoacoustic engines, the regenerator or stack (made of porous material) sandwiched between a pair of (hot and cold) heat exchangers constitutes the so-called thermoacoustic core, where the thermoacoustic energy conversion from heat to acoustic power takes place. The high density acoustic wave can then be used to produce cooling power or to drive an alternator to generate electricity.

Based on the wave type through the stack or regenerator, there are two types of thermoacoustic devices, the standing-wave and travelling-wave devices. The standing-wave thermoacoustic engines have been studied in the last decades. Swift [2] designed and tested a large scale thermoacoustic engine, which uses 13.8 bar helium as the working gas and can deliver 630 W of acoustic power to the external acoustic load, converting the heat (thermal) energy into acoustic power at a thermal efficiency of 9%. There are also several other different size prototypes of standing-wave engines that have been studied by researchers [3][4][5]. However, the standing-wave thermoacoustic engines work on an intrinsically irreversible thermodynamic cycle. Their thermal efficiency ratio of acoustic power produced to heat input has thus far been limited to 20%.

Ceperley [6] pointed out that when a travelling sound wave passes though the regenerator, the heat transfer interaction between the gas and the solid material undergoes a Stirling-like thermodynamic cycle. He also designed a device to test this idea. However, his experimental engine was not able to amplify acoustic power. Yazaki et al [7] first demonstrated such an engine, but at low efficiency. Ceperley [6] and Yazaki [7] realized that this was due to the low acoustic impedance of the working gas, which caused large viscous losses resulting from high acoustic velocities. Much later, based on a compact acoustic network, Scott [8] designed a new type thermoacoustic engine which employs the inherently reversible Stirling in the regenerator and obtained high acoustic impedance to suppress the high acoustic loss. His thermoacoustic Stirling engine demonstrated a thermal efficiency of 30% which is more than 50% higher than any previous thermoacoustic engine.

This paper concerns the design and preliminary testing of a looped-tube travelling-wave thermoacoustic engine. The

A. S. Abduljalil, Z. Yu, A.J. Jaworski (the corresponding author) and L. Shi are with the School of Mechanical, Aerospace and Civil Engineering, University of Manchester, Sackville Street, PO Box 88, Manchester M60 1QD, UK (phone: +44(0)1612754358; e-mail: a.jaworski@manchester.ac.uk).

original purpose of this project was to design a solar driven thermoacoustic machine. The basic idea is that, a travelling wave thermoacoustic engine utilizes solar energy to produce acoustic power, and then uses this acoustic power for either cooling or electricity generation. At the first stage, the engine is constructed using an electrical heater instead of solar power. So far, only the engine part is ready for testing. In this paper, we will briefly show the design, construction and preliminary tests.

II. Experimental Setup

As schematically shown in Fig. 1, a travelling wave thermoacoustic engine was designed as a loop with the thermoacoustic core installed in the appropriate position. DELTAEC, which is a specialized code developed for modeling thermoacoustic devices, has been used for the system design [1]. Air is used as the working gas; the design frequency is 110 Hz. The system has a looped-tube configuration and is made of a stainless steel pipe with the total length of 3 m and an internal diameter of 54 mm. All flanges are ASME grade 316L and class 300. This looped-tube has a constant cross-sectional area throughout. The system was designed to handle a mean pressure of up to 1MPa and a maximum temperature of 750°C at the hottest zone of the tube. The heater, regenerator, and cold heat exchanger are schematically shown in Fig. 1. Fig. 2 shows a photograph of the actual setup.

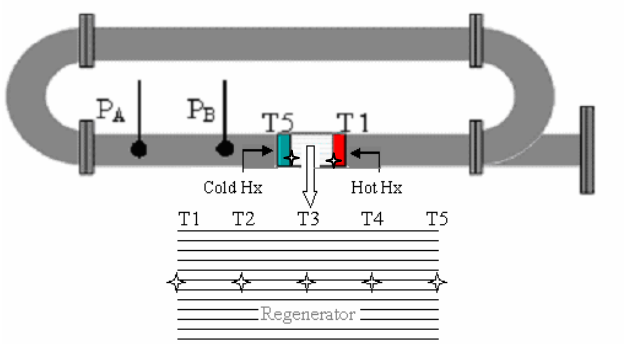

Fig. 1 A schematic diagram of the thermoacoustic engine showing the measurement locations of thermocouples and pressure sensors

The system is equipped with an electric heater that was specially made to supply a uniform heat flux to one end of the regenerator. It was made from Nickel-Chromium resistance wire which was wound around ceramic tubes that serve as supports. Electrical power is supplied to the heater at maximum voltage of 30V and a maximum current of 20A from a DC power supply via a special feedthrough to maintain a good pressure seal.

The regenerator is the main part of the system where thermoacoustic processes take place resulting in conversion of thermal input to acoustic power. Ceramic regenerator, which is made from Corning Cellular Ceramic Catalyst Support, is used as a regenerator. It has square channels with cell density of 900 cpsi (cells per square inch), a hydraulic radius (r_h) of 0.199 mm and porosity (Φ) of 88.7%. The ceramic regenerator is tested in detail to be used later as a benchmark to estimate the performance of other low cost regenerators that will be examined in future.

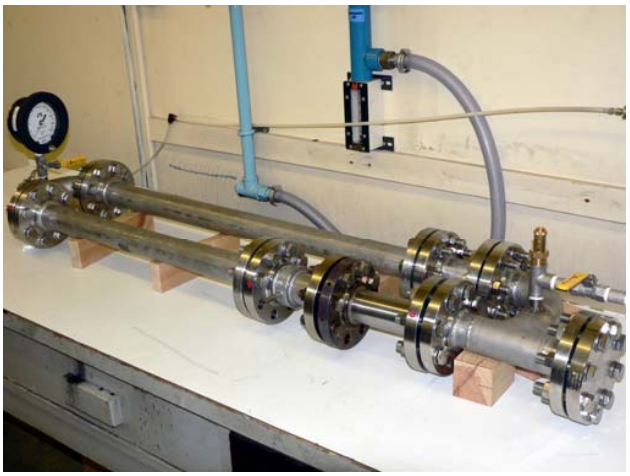

Fig. 2 Looped tube travelling-wave thermoacoustic engine

Fig. 3 The ceramic regenerator

On the cold side of the regenerator, there is a water-jacket that is made for the cooling purpose. Stainless steel scourers with porosity of 95% were placed under the water-jacket and adjacent to the cold end of the regenerator such that the combination of the water-jacket and the stainless steel scourers serves as the cold heat exchanger. On the right end of this engine, there would be a window to receive concentrated sunlight to heat the heater zone when the solar heating concept is investigated in the future. At this stage there is only a blind

flange.

For measurement purposes, a pair of microphones (PCB PIEZOTRONICS model 112A22) is used to measure the oscillating pressure amplitudes as well as the phase angle between the two received signals from the transducers. P-A and P-B marked in Fig. 1 show the locations of these two pressure microphones. The sensitivity of the sensors is 100mV/psi.

Eight Type-K thermocouples (TC-Direct model 408-119) are used to measure the gas temperature along the regenerator and through the two heat exchangers. TC-Direct fittings (model 875-446) were used to feed the thermocouple wires through the tube wall, to ensure a good pressure seal. .

III. Experimental Results and Discussion

The engine has been tested for different mean pressures in the range of pressures from atmospheric to 10 bars.

A. Temperatures Measurement

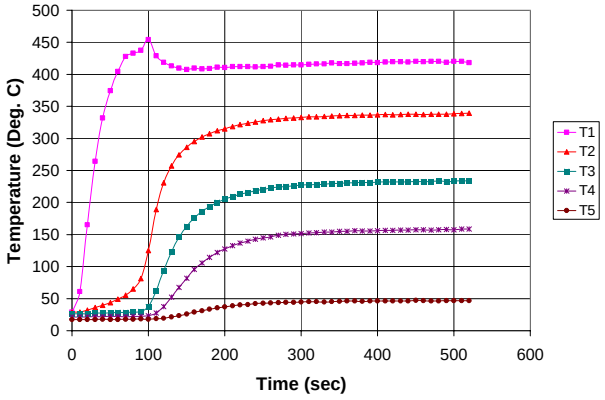

Fig. 4 The temperature evolution in time for five thermocouple locations within the regenerator, plotted from the start of an experiment until 540 seconds, for the mean pressure of 4.4 bar

The rig was tested in three different orientations (horizontal, vertical and inclined with an angle of 15° from the horizontal). By maintaining the same input power to the heater in the three cases, the combined effects of the natural convection and heat conduction in the stainless steel wall on the temperature gradient in the regenerator were tested. It is clear that the temperature gradient is more linear when the rig is in the vertical configuration. Moreover, the temperature difference between the two ends of the regenerator is also higher than for the two other cases, hence, more acoustic power is generated. Moreover, it was noticed that the influence of natural convection shortens the time necessary to start the engine when compared with two other cases.

The engine is hung in an upright position, i.e. the heater is beneath the regenerator and the cold heat exchanger. After turning on the heater, the input power is set to 600 W. The temperatures of T1-T5 increase versus the time as shown in Fig. 4. T1 increases rapidly, after which it reaches a peak, followed by a small decrease. This peak point corresponds to the onset of the pressure oscillation in the resonator. After the onset, the temperatures in the regenerator T2-T5 increase fast, because the oscillation of gas parcels enhances the heat transfer from the heater into the regenerator. When the pressure oscillation reaches stationary conditions, the temperatures in the regenerator also become stationary.

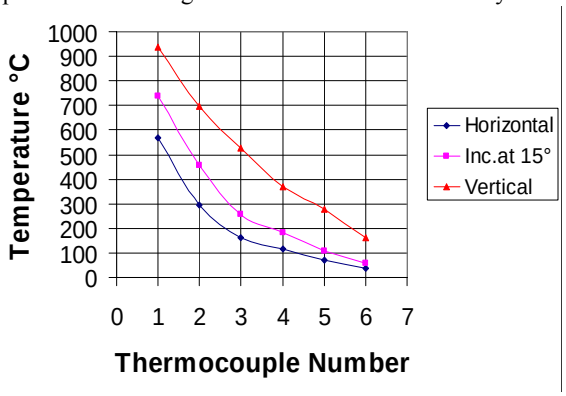

Fig. 5 Temperature gradient along the regenerator in three different orientations of the looped-tube engine

B. Pressure Amplitude Measurement

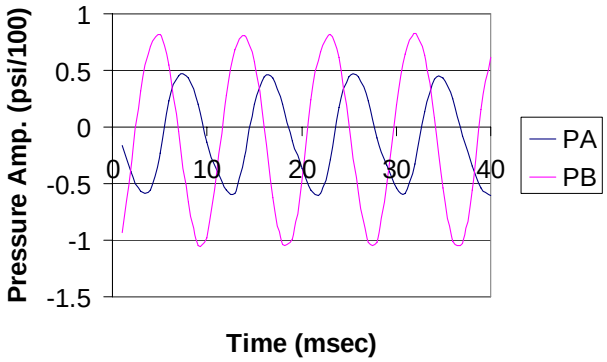

Fig. 6 The pressure oscillation as measured by the two sensors at Pm = 4.4bar

Fig. 6 shows the pressure oscillations measured by the two microphones when the engine reaches a steady state. They are simple sinusoidal waves, with a frequency of 111Hz. In Fig. 6, the two waveforms also indicate the amplitudes and the phase difference between two pressure oscillations. As discussed below, this information can be used to calculate the acoustic power within the resonator.

Fig. 7 shows the pressure amplitude $|p_A|$ (half of the peak-to-peak pressure oscillation) versus different mean pressures. In the figure, the pink line and symbols show the actual pressure amplitude. It can be seen the maximum pressure amplitude appears when the mean pressure is 7 bars. Blue line shows the drive ratio, understood as the amplitude of the pressure oscillations to the mean pressure.

C. Acoustic Power Measurement

Two pressure sensors were placed in short distance of each

other to measure the dynamic pressure variation. The signals indicate the pressure amplitudes, |PA| and |PB|, which, together with the measured phase angle between the two readings, can be used to estimate the generated acoustic transfer as well as the velocity distribution along the looped tube. This method is called the two-microphone measurement method [9].

The following expression for the output acoustic power accounts for the viscous losses near the wall of the tube.

$$\dot{E}_2 = \frac{A}{2\rho_m a \sin(\omega\Delta x/a)} \times \left(\mathrm{Im}\left[p_{1A}\tilde{p}_{1B}\right]\left\{1-\frac{\delta_v}{4r_h}\left[1-\frac{\gamma-1}{\sqrt{\sigma}}+\left(1+\frac{\gamma-1}{\sqrt{\sigma}}\right)\frac{\omega\Delta x}{a}\cot\left(\frac{\omega\Delta x}{a}\right)\right]\right\} + \frac{\delta_v}{8r_h}\left(|p_{1A}|^2-|p_{1B}|^2\right)\left[1-\frac{\gamma-1}{\sqrt{\sigma}}+\left(1+\frac{\gamma-1}{\sqrt{\sigma}}\right)\frac{\omega\Delta x}{a}\csc\left(\frac{\omega\Delta x}{a}\right)\right] \right)$$

In this expression, A is the cross-sectional area, ρ_m is the mean density, a is the speed of sound, ω is the angular frequency, δ_v is the viscous penetration depth, r_h is the hydraulic radius, γ is the specific heat ratio, σ is the Prandtl number, and Δx is the distance between the two sensors.

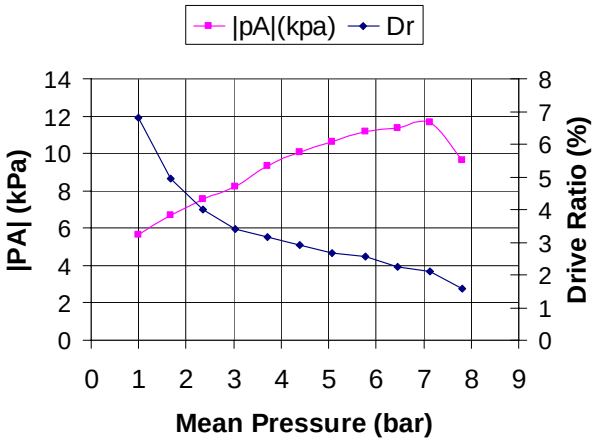

Fig. 7 The measured pressure amplitude by sensor (A) and the associated drive ratio (DA) as they vary with the mean pressure

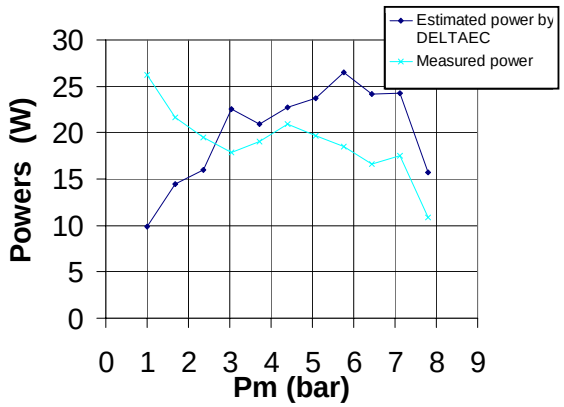

Fig. 8 The estimated acoustic power by DELTAEC compared to the measured values at different mean pressures

Using the readings from the pressure sensors, the acoustic power is estimated from the above expression and then compared with the estimated acoustic power output from the modeling input file that was used in DELTAEC. It can be seen that, at relatively high mean pressure (above 3 bar) the measured power has the same variation as the DELTAEC code estimation. However, at the low mean pressure, the discrepancy is apparent. This is partly due to the difficulty in measuring the phase angle, which results in a bigger error in the measured acoustic power.

IV. Conclusion

The travelling-wave thermoacoustic engine was constructed and successfully tested to generate acoustic power. Some preliminary results were obtained to test the engine performance. The onset temperature differences as well as the temperature evolution in time were measured at different mean pressures. The influence of the natural convection and the conduction through the walls of the tube on the temperatures along the regenerator was studied. The approximate estimation of the acoustic power from the given expression agrees fairly well with the estimated values from DELTAEC. The measured drive ratio was highest at atmospheric pressure; this is due to the effect of the hydraulic radius of the regenerator. In the near future, other regenerators from different porous materials with smaller hydraulic radii will be tested for optimization at higher mean pressures. Moreover, enhancement of the engine performance is expected after the installation of two recently modified heat exchangers for enhanced heat transfer on the two ends of the regenerator.

References

[1] W.C Ward and G.W Swift, "Design environment for low-amplitude thermoacoustic engines," Journal of the Acoustical Society of America, Vol. 95 (6), pp. 3671-3672, 1994.
[2] G.W Swift, "Analysis and performance of a large thermoacoustic engine," Journal of the Acoustical Society of America, Vol. 92 (3), pp. 1551-1563, 1992.
[3] J. R. Olson and G. W. Swift, "A loaded thermoacoustic engine," Journal of the Acoustical Society of America , Vol. 98 (5), pp. 2690-2693.
[4] S. Zhou and Y. Matsubara, "Experimental research of thermoacoustic prime mover ," Cryogenics, Volume 38, Number 8, pp. 813-822, 1998
[5] G. W. Swift, ''Thermoacoustic engines,'' Journal of the Acoustical Society of America, Vol. 84, pp. 1145–1180, 1988.
[6] P. H. Ceperley, "Gain and efficiency of a short travelling wave heat engine," Journal of the Acoustical Society of America, Vol. 77, pp. 1239–1244, 1985.
[7] T. Yazaki, A. Iwata, T. Maekawa, and A. Tominaga, "Travelling Wave Thermoacoustic Engine in a Looped Tube," Physical Review Letters, Volume 81, Number 15: 3128-3131, 1998.
[8] S. Backhaus and G. W. Swift, "A thermoacoustic-Stirling heat engine: Detailed study," Journal of the Acoustical Society of America, Vol. 107, pp. 3148-3166, 2000.
[9] A. M. Fusco, W. C. Ward, and G. W. Swift, ''Two-sensor power measurements in lossy ducts,'' Journal of the Acoustical Society of America , Vol. 84, pp. 2229–2235, 1992.